RSC Advances

PAPER

View Article Online
View Journal | View Issue

Cite this: *RSC Adv.*, 2020, **10**, 13016

Facile electrodeposition of V-doped CoP on vertical graphene for efficient alkaline water electrolysis†

Linh Truong,[a] Sanjib Baran Roy,[a] Sahng-Kyoon Jerng,[b] Jae Ho Jeon,[a] Sunghun Lee[a] and Seung-Hyun Chun*[a]

Received 18th February 2020
Accepted 24th March 2020

DOI: 10.1039/d0ra01538e

rsc.li/rsc-advances

In this work, we demonstrate a highly enhanced electrocatalytic activity of vanadium-doped CoP (V–CoP), directly grafted on a vertical graphene/carbon cloth electrode (VG/CC) by a facile electrochemical deposition method. Impressively, V–CoP/VG/CC exhibited a superior catalytic activity toward the hydrogen evolution reaction (HER) in alkaline solution. Compared to CoP/VG/CC, V-doping decreased the overpotential for HER at 10 mA cm^{-2} by more than half to 40 mV. The new catalyst even outperformed Pt/C beyond 150 mA cm^{-2}. The overpotential for OER at 50 mA cm^{-2} was merely 314 mV, more than 100 mV lower than that of IrO_2. Moreover, our novel catalyst worked as an excellent bifunctional catalyst with a low cell voltage of 1.69 V to achieve a current density of 50 mA cm^{-2}. Detailed characterizations revealed that the V-doping in CoP resulted in improved electrical conductivity and increased active sites. Our findings highlight the significant advantage of V doping on the catalytic activities of CoP, already boosted by VG. Furthermore, concurrent doping with the electrodeposition of catalyst offers a new approach for practical water electrolysis.

The challenges of increasing energy crisis and environmental problems have stimulated scientific exploration into water electrolysis as a sustainable, pure generation of hydrogen to replace fossil fuels. It is highly desirable to develop cost efficient, active and long-term stable catalysts with low overpotentials in the hydrogen evolution reaction (HER) and/or oxygen evolution reaction (OER) for practical applications. Recently, transition metal phosphides (TMPs) such as NiP,[1,2] CoP,[3,4] FeP,[5,6] and MoP[7,8] have received considerable attention because of their superior electrocatalytic activities for hydrogen generation in acidic medium. Later, it turned out that TMPs were also good for the OER in alkaline solution, making these materials more interesting.[9–11] However, the research of bifunctional catalysts out of TMPs for full water splitting is hindered, because their HER and OER performances in the same pH range are still insufficient. Notably most of the non-noble metal based electrocatalysts for OER are inactive and unstable in acid, but work effectively in alkaline medium.[12] Therefore, it is of great significance to improve HER and OER performances of TMPs in alkaline medium to achieve efficient overall water splitting.

Recently, vanadium has been widely used as an excellent foreign dopant to promote alkaline electrocatalytic activities.[13,14] For instance, Guo *et al.* synthesized V-doped Ni_3S_2 nanorod array *via* hydrothermal method to improve HER and OER activities and thus achieved an efficient water splitting performance in 1.0 M KOH.[15] Wen *et al.* facilitated charge carrier migration and enhanced the HER activity of Ni_2P by introducing V.[16] V dopants could also accelerate the OER kinetics of NiFe layered double hydroxides in alkaline medium.[17] However, we note that extensive efforts have been usually taken to introduce V into catalysts, through multi-step and/or time-consuming processes.

Here, we report a successful integration of V into CoP *via* facile electrochemical deposition on a vertical graphene/carbon cloth electrode (VG/CC). We also show that this facile preparation method can take full advantage of the doping effect as revealed in the drastic reduction of overpotential for alkaline HER. Furthermore, V–CoP/VG/CC can be utilized as a bifunctional catalyst for overall water splitting, requiring a low cell voltage of 1.69 V to drive a current density of 50 mA cm^{-2}. Seemingly, the excellent activity comes from the lower charge-transfer resistance and the larger number of active sites caused by V-doping. The underlying mechanism is believed to be a general hetero-atom doping effect as in crystalline systems.

The synthesis process of V–CoP/VG/CC is illustrated in Fig. 1a, including the growth of VG/CC *via* PECVD and the facile electrodeposition of V–CoP on VG/CC. The morphology of V–

[a]*Department of Physics, Sejong University, Seoul 05006, Korea. E-mail: schun@sejong.ac.kr; Fax: +82 2 3408 4316*

[b]*Graphene Research Institute, Sejong University, Seoul 05006, Korea*

† Electronic supplementary information (ESI) available: Experimental section. See DOI: 10.1039/d0ra01538e

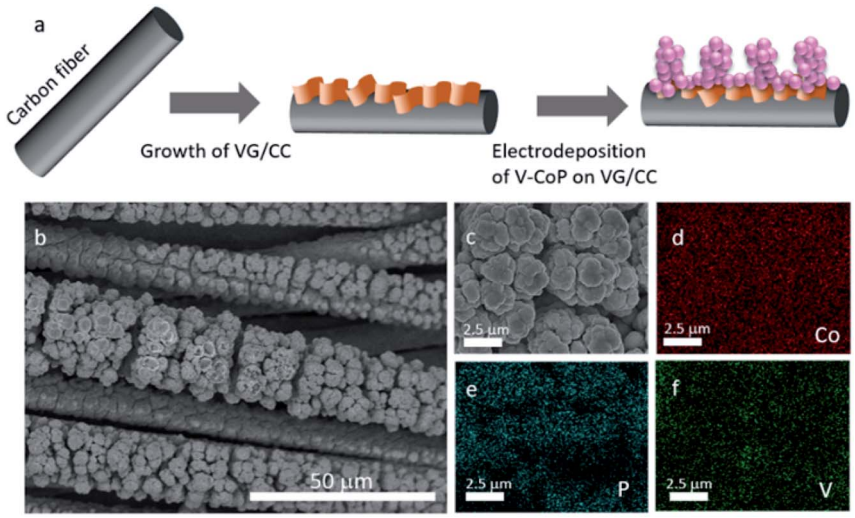

Fig. 1 (a) Schematic representation of the V–CoP/VG/CC fabrication process. (b) Low- and (c) high-magnification SEM images of V–CoP/VG/CC. EDS elemental mapping images of (d) Co, (e) P, and (f) V.

CoP/VG/CC was investigated by scanning electron microscopy (SEM). The entire surface of CC (Fig. S1a†) was fully covered by nanoscale VG (Fig. S1b†). The morphology of V–CoP was strongly dependent on the morphology of the substrate. Under the same electrodeposition conditions, V–CoP submicron particles with a diameter around 600–700 nm were observed on CC (Fig. S1c†) while V–CoP cauliflower-like structures were obtained on VG/CC substrate (Fig. 1b, c and S1d†). Besides, the concentration of V in the electrodeposition solution could make a difference in the morphology of V–CoP/VG/CC. Fig. S2† shows the low- and the high-magnification images of V–CoP/VG/CC prepared with 5 mM and 15 mM VCl_3, where rather rounded microstructures were observed. As we will show later, these differences in the morphology affect the HER and OER performances since the rougher catalytic surface provides the larger active sites for electrocatalytic reactions.[18] The elemental mapping results in Fig. 1d–f confirmed the distributions of Co, P, and V elements throughout the V–CoP/VG/CC cauliflower-like structures. The energy dispersive spectroscopy (EDS) analysis in Fig. S3† showed the composition ratio of V : Co : P in V–CoP/VG/CC (for 5 mM vanadium reagent) to be around 0.4 : 9.8 : 10.3, indicating a V-doping dosage of 4%. By changing the concentration of added VCl_3 during the electrodeposition process, the doping ratio can be controlled. X-ray photoelectron spectroscopy (XPS) spectra in C (1s), Co (2p), P (2p), and V (2p) regions confirmed the formation of V–CoP on VG/CC as shown in Fig. S4.†

To evaluate the influence of vanadium dopant on HER activities of CoP, bare CC, VG/CC, Pt/C, CoP/VG/CC, and V–CoP/VG/CC were tested in 1.0 M KOH solution. As shown in Fig. 2a, the Pt/C presented as a representative catalyst for HER with near zero overpotential while the bare CC and VG/CC showed very poor HER performances. To approach a current density of 10 mA cm^{-2}, CC and VG/CC required an overpotential of 305 and 285 mV, respectively. We have shown previously that CoP on VG/CC was an outstanding catalyst with low overpotentials.[19] Briefly, the nanoscale rough surface of VG enables rapid disengagement of gas bubbles, called superaerophobic property, in addition to the general benefits of carbon-based materials, resulting in enhanced catalytic activities.[20–22] Here, we found that such enhancement was further amplified by the addition of V. We observed that the introduction of V into CoP reduced the overpotential from 93 mV (for CoP/VG/CC) to 40 mV (for V–CoP/VG/CC) at the current density of 10 mA cm^{-2}. This HER performance is far better than those of other electrocatalysts with transition metals as shown in Table S1.† V–CoP/VG/CC even required smaller overpotentials than Pt/C to generate high current densities beyond 150 mA cm^{-2}. Moreover, the novel V–CoP/VG/CC catalyst possessed the smallest Tafel slope value of merely 40 mV dec^{-1}, reaching the

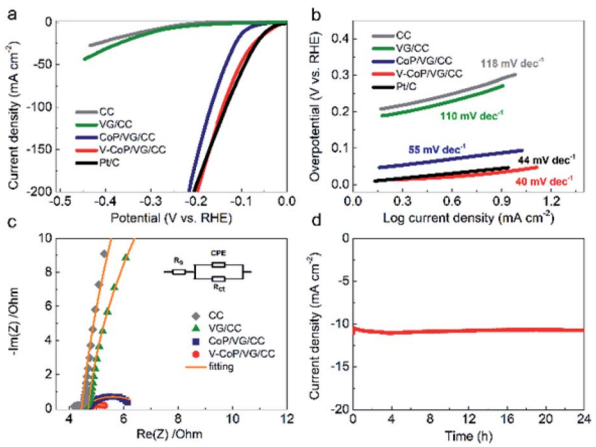

Fig. 2 Electrochemical HER activity of V–CoP/VG/CC in 1.0 M KOH (a) polarization curves of bare CC, VG/CC, CoP/VG/CC,[19] V–CoP/VG/CC, and Pt/C electrode. (b) The corresponding Tafel slopes. (c) Nyquist plots; the inset is a schematic model circuit used for analysis. (d) The time-dependent current density of V–CoP/VG/CC under 40 mV during 24 h in 1.0 M KOH.

theoretical value of Heyrovsky process (Fig. 2b). This indicates that the HER activity of CoP was greatly improved after V-doping. The electrochemical impedance spectroscopy (EIS) measurement was carried out to estimate the charge transfer resistance of catalysts at the interface of electrode and electrolyte. The charge transfer resistance (R_{ct}) could be determined from the diameter of EIS semicircle.[23] As can be seen in Fig. 2c, R_{ct} of V–CoP/VG/CC (1.4 Ω) was much smaller than that of CoP/VG/CC (2.3 Ω), indicating that much faster catalytic kinetics was achieved by V-doping. The stability test of V–CoP/VG/CC was also conducted under a constant overpotential of 40 mV for 24 h to evaluate the feasibility of practical applications. Fig. 2d shows a negligible fluctuation in the current density of 10 mA cm^{-2}, indicating V–CoP/VG/CC has an excellent stability in alkaline medium.

We further investigated the OER catalytic activities of VG/CC, CC, IrO_2, CoP/VG/CC, and V–CoP/VG/CC in 1.0 M KOH solution. As expected, VG/CC and CC did not display appreciable current densities below 1.6 V, while IrO_2 and CoP/VG/CC showed the same overpotential of 300 mV at 10 mA cm^{-2}. Clearly, the OER activity of V–CoP/VG/CC was far superior to those of IrO_2 and CoP/VG/CC (Fig. 3a). The anodic peak at around 1.4 V has been commonly found in the Co-based electrocatalysts[24] and could be assigned to the oxidation peak of Co. The Tafel slope value of V–CoP/VG/CC was smaller than those of other catalysts compared here (Fig. 3b). Furthermore, the EIS measurements revealed that R_{ct} of V–CoP/VG/CC (1.5 Ω) was much smaller than those of CoP/VG/CC (5.6 Ω), VG/CC (8.5 Ω) and CC (10 Ω) (Fig. 3c), suggesting a faster catalytic kinetic process of V–CoP/VG/CC. The time-dependent current density, tested at the overpotential of 314 mV for 24 h, showed that our novel V–CoP/VG/CC catalyst possessed a long-term stability with merely 6% loss (Fig. 3d). As V–CoP/VG/CC possessed outstanding HER and OER activities with low overpotentials, fast catalytic kinetics and durability, bifunctional catalyst performance of V–CoP/VG/CC was investigated in 1.0 M KOH. When V–CoP/VG/CC catalysts were used as both cathode and anode in a two-electrode configuration, a low cell voltage of 1.69 V was demanded to generate a current density of 50 mA cm^{-2} (Fig. 4a). Furthermore, the stability was also outstanding even at this high current density, maintaining over 90% after 24 h test as shown in Fig. 4b.

To further understand the enhanced activity of V–CoP/VG/CC over CoP/VG/CC, double layer capacitance (C_{dl}) was compared as a measure of effective surface area. Fig. S5a and c† show the CV curves of CoP/VG/CC and V–CoP/VG/CC at different scan rates (20–100 mV cm^{-2}), respectively. The hysteresis increases as the scan rate, and the dependence gives C_{dl}. Obviously, the C_{dl} value of V–CoP/VG/CC (95 mF cm^{-2}) was larger than that of CoP/VG/CC (72 mF cm^{-2}) (Fig. S5b and d†), implying more exposed active sites per unit area for V–CoP/VG/CC. Accordingly, all the characterizations support the positive influence of vanadium doping on the electrocatalytic activities of CoP.

The catalytic activity of V–CoP/VG/CC catalyst could be optimized by varying the applied current density or the amount of VCl_3 during the electrodeposition. The electrocatalytic performances of as-prepared V–CoP/VG/CC (10 mM VCl_3) with different applied current densities of 0.05 A cm^{-2} and 0.1 A cm^{-2} were evaluated through HER and OER in 1.0 M KOH, and the V–CoP/VG/CC – 0.1 A cm^{-2} displayed the better HER and OER as confirmed in Fig. S6a and b.† Similarly, Fig. S7a and b† compare the HER and OER performances of V–CoP/VG/CC with different amounts of vanadium reagents (5, 10, and 15 mM VCl_3). The V–CoP/VG/CC with 10 mM VCl_3 possessed the best electrocatalytic performance for both HER and OER, as expected from the rough microstructure (Fig. 1).

It is acknowledged that the H_2O adsorption and the H adsorption/desorption are central processes in the alkaline HER.[25,26] Chen *et al.* argued that V-doping could improve the HER performance of Co_4N in alkaline medium as more electrons filled the anti-bonding states and the d-band center was downshifted from the Fermi level, which in turn weakened the interaction between the adsorbate and the catalyst surface. In addition, density functional theory (DFT) calculations showed that the free energy of adsorbed H (ΔG_{H^*}) was reduced to less

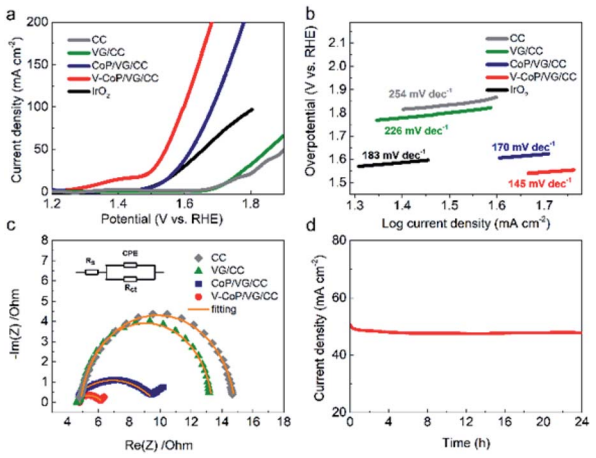

Fig. 3 Electrochemical OER activity of V–CoP/VG/CC in 1.0 M KOH (a) polarization curves of bare CC, VG/CC, CoP/VG/CC,[19] V–CoP/VG/CC, and IrO_2 electrode. (b) The corresponding Tafel slopes. (c) Nyquist plots; the inset is a schematic model circuit used for analysis. (d) The time-dependent current density of V–CoP/VG/CC under 314 mV during 24 h in 1.0 M KOH.

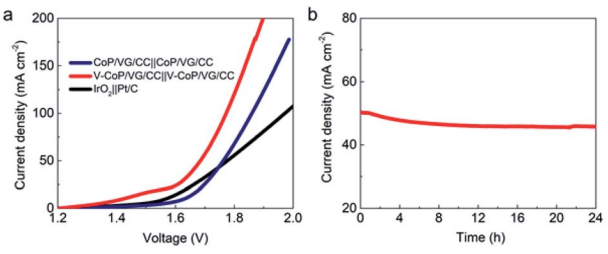

Fig. 4 (a) Bifunctional water electrolysis tested in 1.0 M KOH.[19] (b) The time-dependent current density of using two V–CoP/VG/CC electrodes at a constant cell voltage of 1.69 V during 24 h in 1.0 M KOH.

than half after V-doping, providing a reasonable explanation to elucidate the enhanced alkaline HER.[27]

Moreover, V-doping could lower the overpotential of Co-based catalyst toward OER. Liu *et al.* provided DFT calculations of V-doped CoOOH model, offering valuable insights for OER enhancements. Three sites (Co site on pristine CoOOH, Co site on V-doped CoOOH, and V site on V-doped CoOOH) were considered, and the OER process *via* intermediate steps was evaluated. It turned out that the free energy landscape was affected significantly because of doping, and the Co site adjacent to V gave the smallest overpotential at the rate limiting step.[28] Yan *et al.* also performed similar calculations and obtained the same conclusions, confirming the effect of V to enhance the OER activity.[29]

The above arguments are closely related to our experiments. First, although DFT calculations were obviously performed for lattice structures, we expect a similar free energy gain for amorphous hetero-systems because of the local substitution effect. Second, for HER, the d-band engineering should be a general trend because of the smaller electron affinity of V than that of Co. Finally, as CoP transforms into CoOOH during the OER process, the effect of V-doping on OER is equally applicable in our system.[30,31] Thus, we believe that the doping enhanced HER and OER should be a general aspect of amorphous V–CoP as well as crystalline counterpart.

In summary, we have designed a simple electrodeposition method to synthesize V–CoP/VG/CC cauliflower-like structure as an active bifunctional catalyst for water splitting in alkaline solution. The presence of vanadium dopants into CoP reduced the charge transfer resistance and acquired addition catalytic active surface sites, which were beneficial for promoting the electrocatalytic activities. As a result, the as-prepared V–CoP/VG/CC exhibited improved catalytic activities with overpotentials of 40 mV at 10 mA cm^{-2} (HER), 314 mV at 50 mA cm^{-2} (OER), and a low cell voltage of 1.69 V (full water splitting) to afford the current density of 50 mA cm^{-2}, along with an excellent stability in alkaline condition. Our work demonstrates that the electrocatalytic activity of earth abundant metal-based catalyst can be easily accelerated by facile cation-doping and chemically-stable support of suitable nanostructure.

Conflicts of interest

There are no conflicts to declare.

Acknowledgements

This work supported by National Research Foundation of Korea (NRF) funded by the Ministry of Science and ICT and the Ministry of Education (No. 2016R1E1A1A01942649, 2018R1A5A6075964, 2018K1A4A3A01064272, and 2018R1D1A1B07048109).

References

1 A. R. J. Kucernak and V. N. Naranammalpuram Sundaram, *J. Mater. Chem. A*, 2014, **2**, 17435–17445.
2 E. J. Popczun, J. R. McKone, C. G. Read, A. J. Biacchi, A. M. Wiltrout, N. S. Lewis and R. E. Schaak, *J. Am. Chem. Soc.*, 2013, **135**, 9267–9270.
3 L. Ma, X. Shen, H. Zhou, G. Zhu, Z. Ji and K. Chen, *J. Mater. Chem. A*, 2015, **3**, 5337–5343.
4 F. H. Saadi, A. I. Carim, E. Verlage, J. C. Hemminger, N. S. Lewis and M. P. Soriaga, *J. Phys. Chem. C*, 2014, **118**, 29294–29300.
5 J. Tian, Q. Liu, Y. Liang, Z. Xing, A. M. Asiri and X. Sun, *ACS Appl. Mater. Interfaces*, 2014, **6**, 20579–20584.
6 D. Li, Q. Liao, B. Ren, Q. Jin, H. Cui and C. Wang, *J. Mater. Chem. A*, 2017, **5**, 11301–11308.
7 P. Xiao, M. A. Sk, L. Thia, X. Ge, R. J. Lim, J.-Y. Wang, K. H. Lim and X. Wang, *Energy Environ. Sci.*, 2014, **7**, 2624–2629.
8 J. M. McEnaney, J. C. Crompton, J. F. Callejas, E. J. Popczun, A. J. Biacchi, N. S. Lewis and R. E. Schaak, *Chem. Mater.*, 2014, **26**, 4826–4831.
9 Y. Yan, B. Zhao, S. C. Yi and X. Wang, *J. Mater. Chem. A*, 2016, **4**, 13005–13010.
10 J. Ryu, N. Jung, J. H. Jang, H. Kim and S. J. Yoo, *ACS Catal.*, 2015, **5**, 4066–4074.
11 S. Fu, C. Zhu, J. Song, M. H. Engelhard, X. Li, D. Du and Y. Lin, *ACS Energy Lett.*, 2016, **1**, 792–796.
12 M. Jamesh and X. Sun, *J. Power Sources*, 2018, **400**, 31–68.
13 Y. Qu, M. Yang, J. Chai, Z. Tang, M. Shao, C. T. Kwok, M. Yang, Z. Wang, D. Chua, S. Wang, Z. Lu and H. Pan, *ACS Appl. Mater. Interfaces*, 2017, **9**, 5959–5967.
14 X. Shang, K.-L. Yan, Y. Rao, B. Dong, J.-Q. Chi, Y.-R. Liu, X. Li, Y.-M. Chai and C.-G. Liu, *Nanoscale*, 2017, **9**, 12353–12363.
15 J. Guo, K. Zhang, Y. Sun, Q. Liu, L. Tang and X. Zhang, *Inorg. Chem. Front.*, 2019, **6**, 443–450.
16 L. Wen, J. Yu, C. Xing, D. Liu, X. Lyu, W. Cai and X. Li, *Nanoscale*, 2019, **11**, 4198–4203.
17 P. Li, X. Duan, Y. Kuang, Y. Li, G. Zhang, W. Liu and X. Sun, *Adv. Energy Mater.*, 2018, **8**, 1703341.
18 J. R. Zeng, M. Y. Gao, Q. B. Zhang, C. Yang, X. T. Li, W. Q. Yang, Y. X. Hua, C. Y. Xu and Y. Li, *J. Mater. Chem. A*, 2017, **5**, 15056–15064.
19 L. Truong, S.-K. Jerng, S. B. Roy, J. H. Jeon, K. Kim, K. Akbar, Y. Yi and S.-H. Chun, *ACS Sustainable Chem. Eng.*, 2019, **7**, 4625–4630.
20 S. Mao, Z. Wen, S. Ci, X. Guo, K. Ostrikov and J. Chen, *Small*, 2015, **11**, 414–419.
21 Z. Zhang, W. Li, M. F. Yuen, T.-W. Ng, Y. Tang, C.-S. Lee, X. Chen and W. Zhang, *Nano Energy*, 2015, **18**, 196–204.
22 K. Akbar, S. Hussain, L. Truong, S. B. Roy, J. H. Jeon, S. K. Jerng, M. Kim, Y. Yi, J. Jung and S. H. Chun, *ACS Appl. Mater. Interfaces*, 2017, **9**, 43674–43680.
23 J. Wang, F. Xu, H. Jin, Y. Chen and Y. Wang, *Adv. Mater.*, 2017, **29**, 1605838.
24 Z.-J. Jiang and Z. Jiang, *Sci. Rep.*, 2016, **6**, 27081.
25 J. Zhang, T. Wang, P. Liu, Z. Liao, S. Liu, X. Zhuang, M. Chen, E. Zschech and X. Feng, *Nat. Commun.*, 2017, **8**, 15437.
26 X. Jia, Y. Zhao, G. Chen, L. Shang, R. Shi, X. Kang, G. I. N. Waterhouse, L. Wu, C. Tung and T. Zhang, *Adv. Energy Mater.*, 2016, **6**, 1502585.

27 Z. Chen, Y. Song, J. Cai, X. Zheng, D. Han, Y. Wu, Y. Zang, S. Niu, Y. Liu, J. Zhu, X. Liu and G. Wang, *Angew. Chem., Int. Ed.*, 2018, **57**, 5076–5080.
28 J. Liu, Y. Ji, J. Nai, X. Niu, Y. Luo, L. Guo and S. Yang, *Energy Environ. Sci.*, 2018, **11**, 1736–1741.
29 Y. Cui, Y. Xue, R. Zhang, J. Zhang, X. Li and X. Zhu, *J. Mater. Chem. A*, 2019, **7**, 21911–21917.
30 C. Guan, W. Xiao, H. Wu, X. Liu, W. Zang, H. Zhang, J. Ding, Y. P. Feng, S. J. Pennycook and J. Wang, *Nano Energy*, 2018, **48**, 73–80.
31 G. Zhang, B. Wang, J. Bi, D. Fang and S. Yang, *J. Mater. Chem. A*, 2019, **7**, 5769–5778.